Eur. Phys. J. B **31**, 545–551 (2003)
DOI: 10.1140/epjb/e2003-00064-0

THE EUROPEAN PHYSICAL JOURNAL B

Preparation and characterization of cobalt-based nanostructured materials

G. Carotenuto[1,a], L. Pasquini[2], E. Milella[1], M. Pentimalli[3], R. Lamanna[4], and L. Nicolais[1]

[1] Istituto per i Materiali Compositi e Biomedici. Consiglio Nazionale delle Ricerche. Piazzale Tecchio, 80 - 80125, Napoli, Italy
[2] Dipartimento di Fisica. Università di Bologna e INFM V.le Berti-Pichat 6/2I - 40127, Bologna, Italy
[3] MAT-COMP. ENEA C.R. Brindisi S.S. 7 Appia Km 713.7 - 72100, Brindisi, Italy
[4] BIOTEC-AGRO. ENEA C.R. Trisaia S.S. 106 Jonica Km 419.5 - 75026, Rotondella, Matera, Italy

Received 27 September 2002
Published online 6 March 2003 –

Abstract. Nano-sized cobalt clusters passivated by alkane-thiol molecules were obtained by the action of concentrated thiol solutions on micrometric cobalt particles. Thiol molecules caused an erosive process on the metal grains with the consequent formation of nano-sized metal debris and cobalt thiolate as by-product. The final material microstructure was composed by cobalt clusters embedded into a continuum cobalt thiolate matrix. Depending on the thiol molecule length, the material texture ranged from rubbery to waxy. These new types of nanocomposite materials were found to be crystalline, thermally stable up to ca. 300 °C, intensely red colored, and high hydrophobic. In addition, they generated polymeric structures when dissolved in non-polar solvents.

PACS. 68.43.-h Chemisorption/physisorption: adsorbates on surfaces – 81.07.Pr Organic-inorganic hybrid nanostructures – 81.16.Be Chemical synthesis methods

1 Introduction

The chemisorption of thiol molecules on metal surfaces has been widely studied because of its relevance both in the desulphuration chemistry [1] and in the formation of self-assembled monolayers (SAM) [2]. Furthermore, the passivation of metal nano-crystals by organic thiols is a very important process since it allows to prevent phenomena such as aggregation and surface oxidation/contamination of small metal particles [3]. Thiol-derivatized metal clusters are special compounds used in the fabrication of advanced functional materials for application in different technological fields (*e.g.*, single-electron transistors, high-density recording media, sensors, optical devices, etc.) [4–12].

Organic thiols undergo S-H bond dissociation to form thiolates on most transition metal surfaces [1]. However, the thiol-metal reactivity is strongly dependent on the type of metal. In fact, metals like Pb, Co, and Ni are completely dissolved by the action of pure liquid thiols. On the other side, the reaction of Au, Ag and Pd powders with thiols only involves the metal surface. When a coarse cobalt powder is treated at room temperature with an alcoholic solution of thiols (dilute or moderately concentrated), only the surface of cobalt grains is involved in the reaction. A slow erosion of the coarse metal grains is observed when the chemical treatment is made by pure liquid thiols. Actually, by using a fine cobalt powder, the reaction time can be reduced while the reaction yield significantly increases. In fact, metals with a fine grain size are characterized by a pronounced chemical reactivity. This is due to the high percentage of surface atoms and to the presence of a large quantity of atoms with a low coordination number on the grain surface [3]. The high surface reactivity which characterizes fine cobalt powders allows the chemical reaction with thiols to proceed quantitatively in only a few minutes at room temperature. The reaction should evolve according to the following scheme:

$$\mathrm{Co} + 2\mathrm{R} - \mathrm{SH} \rightarrow \mathrm{Co(SR)_2} + \mathrm{H_2}. \qquad (1)$$

As shown hereinafter, under particular experimental conditions, the cobalt grains are not completely converted to cobalt thiolate, $\mathrm{Co(SR)_2}$. A large amount of quasi-spherical nano-sized cobalt clusters passivated by the thiol molecules, $\mathrm{Co}_n(\mathrm{SR})_m$ with $n \gg m$, rather result as reaction products. In particular, the products of the chemical reaction of dodecanethiol (*i.e.*, $\mathrm{C_{12}H_{25}SH}$) and octadecanethiol (*i.e.*, $\mathrm{C_{18}H_{37}SH}$) solutions with freshly prepared micrometric cobalt particles were characterized. Monodisperse spherical cobalt particles with a size of a few microns were prepared by the polyol process which is a well-known technique for the synthesis of micron/sub-micron sized spherical particles of easy-reducible metals (*e.g.*, Co, Ni, Ag, etc.) [13].

[a] e-mail: giancaro@unina.it

In the present paper the properties of these novel nanostructured materials were studied with a number of characterization techniques such as atomic force microscopy (AFM), wide-angle X-ray diffraction (XRD), scanning electron microscopy (SEM), optical spectroscopy (UV-VIS-NIR), differential scanning calorimetry (DSC), thermogravimetric (TG) analysis and nuclear magnetic resonance (NMR).

2 Experimental

2.1 Material preparation

Micrometric cobalt particles were obtained by reduction of cobalt ions. Cobalt hydroxide ($Co(OH)_2$, Aldrich 99.8%) and di(ethylene glycol) (DEG) ($O(CH_2CH_2OH)_2$, Aldrich 98%) were used as metal precursor and reductant, respectively. These chemicals were not further purified before their use. The powder (4 g), which resulted scarcely soluble in glycol, was accurately dispersed in a little amount (ca. 10 ml) of DEG, using a sonication bath. This quantity was quickly added to 400 ml of refluxing DEG (280 °C). After 20 min the reactive mixture appeared black since of the metal reduction to the zero-valence state and the reaction was stopped by cooling down the reactive mixture. The reaction was performed under fluxing nitrogen in order to avoid metal oxidation. A monodispersed sample of spherical particles with an average size of 1.3 μm ($\sigma = 3\%$) was obtained.

The as-obtained cobalt suspension was treated at room temperature with a concentrated DEG solution of octadecanethiol (Aldrich, 98%) or an excess of liquid dodecanethiol (Aldrich, 98%). The reaction time was ranging from 15 min to 4 h. At the end of the reaction, a viscous system containing a finely dispersed brown precipitate resulted. The reaction products and the thiol excess were separated from DEG by addition of cyclohexane. The reaction product, dissolved in the hydrocarbon phase, produced an intensely reddish-colored solution. Most of the product constituted a dark-red gel phase segregated at bottom of the hydrocarbon solution. A large quantity of cyclohexane, under stirring and eventually heating were required to dissolve all the product. The obtained solution was dried and the solid washed with acetone. Then, the product was accurately purified by dissolution in chloroform and re-precipitation by acetone addition. After purification it dissolved much quickly, without gel-phase formation.

2.2 Instruments

Atomic Force Microscope (Digital Instruments NanoScope – Multimode 3A) was used in the Tapping mode configuration. The specimens were prepared by placing a small drop of a dilute hydrocarbon solution of Co-$C_{12}H_{25}SH$ on a pyrolytic graphite substrate. The solvent was quickly removed by heating with an IR lamp. X-ray diffraction measurements were performed with a Rigaku DMAX-IIIC goniometer using Cu-K_α radiation ($\lambda = 0.154056$ nm) and a pyrolytic graphite monochromator in the diffracted beam. The goniometer was operated in the standard Bragg-Brentano $\theta/2\theta$ parafocusing geometry. SEM micrograph of cobalt powder and metallized nanocomposite films were obtained by a scanning electron microscope (Cambridge S360). Differential scanning calorimetry (TA-Instrument Mod.Q100) and thermogravimetric analysis (TA-Instrument Mod.Q500) were carried out under inert atmosphere of dry nitrogen. Optical spectra were recorded by an UV-visible spectrophotometer (HP-8453), equipped with a Peltier apparatus to control the sample temperature.

Different NMR techniques were used to study the behavior of the Co-$C_{12}H_{25}SH$ system in solution. A concentrated sample (sample A) was prepared by dissolving 10mg of a Co-$C_{12}H_{25}SH$ film in 0.5 ml of $CDCl_3$ (Aldrich, 99.98%). Two other samples were obtained by diluting sample A in the ratios 1:4 (sample B) and 1:6 (sample C), respectively. Pure $C_{12}H_{25}SH$ (Aldrich, 98%) in $CDCl_3$, 50% by volume (sample D) was used as reference sample. NMR measurements were carried out on a Bruker 600Avance Spectrometer operating at 14T magnetic field, equipped with a broad band probe (BBO) and a high resolution magic angle spinning (HR-MAS) probe. Static ^{1}H NMR spectra of samples A, B, and C were taken by the BBO probe at 27 °C. MAS spectra of all the samples were acquired by the ^{1}H HR-MAS using 4 mm HR-MAS rotors with 12 μl spherical sample volume. The proton HR-MAS spectra were collected at 27 °C with a $\pi/2$ pulse of 5 μs, a relaxation delay (RD) of 5 s and a spinning rate (SR) of 5 kHz. In particular, the spectra of Co-$C_{12}H_{25}SH$ samples were acquired using a diffusion filtered sequence (LED 1D) with a time of flight $\Delta = 100$ ms and a gradient pulse duration $\delta = 1$ ms. The use of the diffusion filter allows to observe signals exclusively from slow diffusing molecules thus eliminating the spurious signals from small contaminants present in the solvent. Diffusion measurements were carried out by means of a Longitudinal Eddy current Delay (LED) pulse sequence with bipolar sine shaped gradient pulses of different intensities [14,15]. The gradient amplitude (g) ranged from 1.6 to 28.9 gauss cm^{-1} in 32 constant steps. The time of flight and the gradient pulse duration were $\Delta = 100$ ms and $\delta = 2$ ms, respectively. The delay between the two bipolar gradient pulses was $\tau = 400$ μs. Eight transients were co-added with a recycle delay of 10 s. Gradient calibration was accomplished through the self- diffusion coefficient of water at 25 °C [16].

3 Results

The alcoholic reduction of cobalt ions produced micrometric cobalt particles whose microstructure was imaged by scanning electron microscopy. As shown in Figure 1a, the particles were perfectly spherical, monodisperse and with an average size of 1.3 microns ($\sigma = 3\%$).

The morphology of nano-sized Co clusters produced by the action of concentrated dodecanethiol solutions on the micrometric cobalt particles, has been imaged by atomic

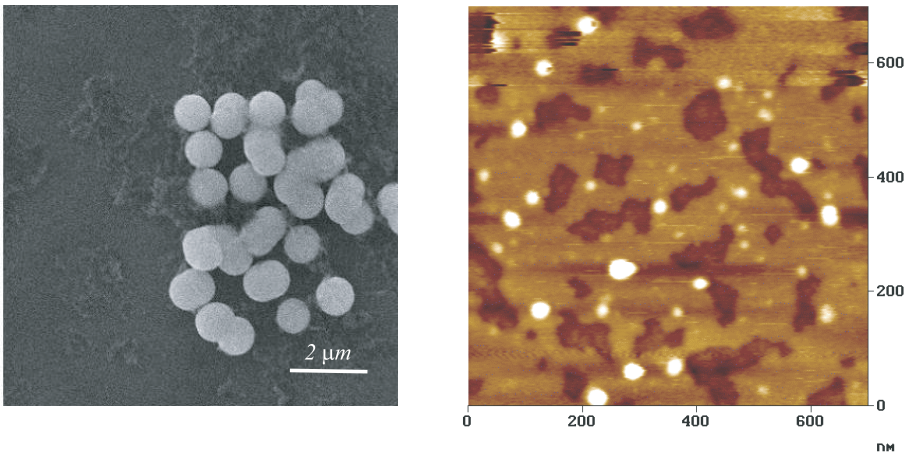

Fig. 1. (a) SEM-micrograph of micrometric cobalt particles and (b) AFM image showing the microstructure of a Co-$C_{12}H_{25}SH$ sample.

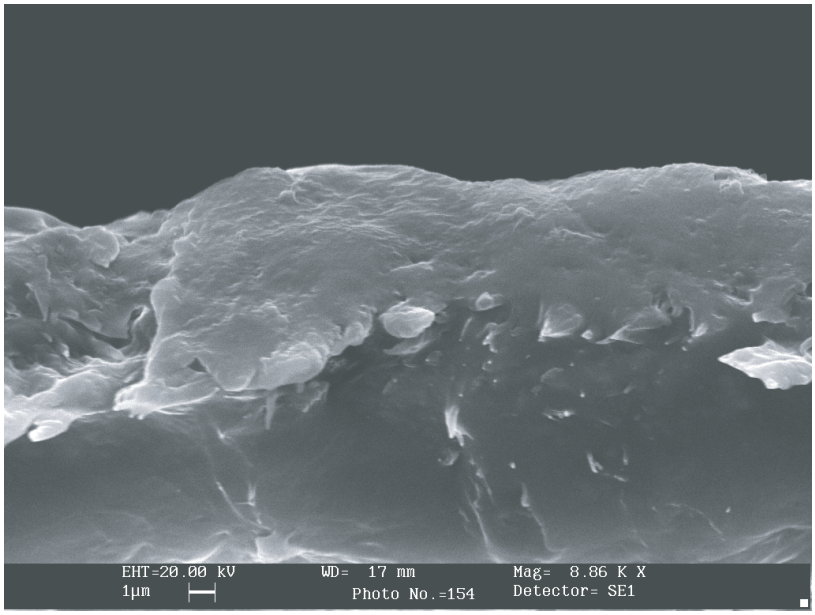

Fig. 2. SEM-micrograph of the Co-$C_{12}H_{25}SH$ film cross-section.

force microscopy. Figure 1b shows the typical microstructure of a Co-$C_{12}H_{25}SH$ sample. The picture evidences the presence of pseudo-spherical particles with an average size of ca. 20 nm, embedded into a continuum phase which microstructure is not resolved in the AFM image. The spherical particles are probably Co(0) nano-crystals passivated by dodecanethiol molecules, produced during the erosive process. The continuum phase embedding the particles should be made of $Co(SC_{12}H_{25})_2$, which amount in the system is a function of the erosion time. In general, the particle size distribution of produced nano-crystallites was broad and the average value was depending on the reaction time. In particular, for treatments with absolute dodecanethiol shorter than 5 min there were not evidences of erosion processes and probably the only effect was a coating of particle surface by chemisorbed thiol molecules. Erosion effects were clearly visible for treatments longer than 15 min, since cobalt crystallites were reduced to a nanometer scale range and an embedding thiolate phase appeared. As an example, the crystallites shown in Figure 1b (average size of 20 nm and σ of 30%) resulted at end of a 40 min treatment. A complete conversion to cobalt thiolate was achieved at room temperature by treatments of 4 h with absolute dodecanethiols.

The dry Co-$C_{18}H_{37}SH$ was a waxy powder unable to produce coherent films by slow solvent evaporation. Whereas the Co-$C_{12}H_{25}SH$ formed flexible, mechanically robust, high-quality films. These films had a rubbery consistence and a light golden surface coloration. Their microstructure was investigated by scanning electron microscopy. The cross-section of Co-$C_{12}H_{25}SH$ films resulting from 40 min treatment with absolute thiol at room temperature is shown in Figure 2. As visible, the films were very uniform and did not show morphological defects (*e.g.*, cracks, fractures, pores, etc.), some craters were visible on the film top-view.

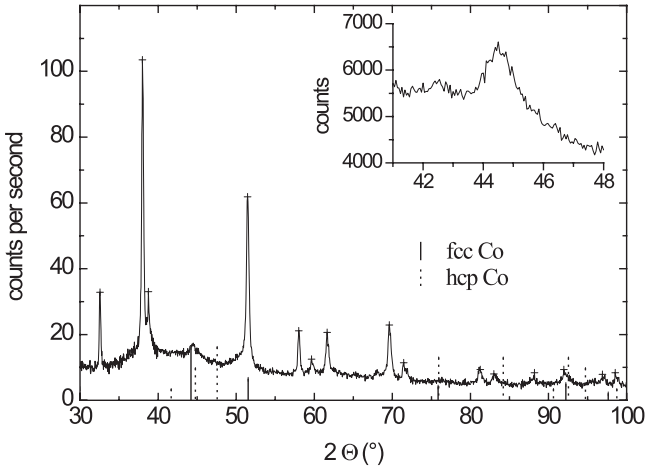

Fig. 3. X-ray diffraction profile of a Co-$C_{12}H_{25}SH$ sample. The solid and dotted vertical lines at the bottom of the layer represent the positions and relative intensities, as reported in the literature, of the peaks pertaining to fcc and to hcp cobalt, respectively. The inset shows an enlarged view of the peak identified as the (111) Bragg reflex of fcc Co.

The wide-angle XRD profile of the Co-$C_{12}H_{25}SH$ exhibited a series of reflexes, labeled by crosses (+) in Figure 3, whose line-width was quite narrow, close to the instrumental resolution of the diffractometer. This observation indicated that the size of the coherently diffracting domains was above 50 nm. Their angular positions did not match the ones characteristic of face centered cubic (fcc) and hexagonal close-packed (hcp) cobalt, represented by solid and dotted vertical lines in the bottom of Figure 2, respectively. The two observations altogether suggest that these peaks were originated by crystallized regions with poor metallic cobalt content and therefore they were probably produced by the crystallization of thiolate molecules (*i.e.*, $Co(SC_{12}H_{25})_2$). In addition, a broad peak centered around 44.45°, identified as the (111) Bragg reflex of fcc cobalt, was observed. A trace of the (220) peak was also visible at 75.8°. The other reflexes are probably too weak to be detected on the background. No traces of the hcp phase was detected in the spectrum. An enlarged view of the (111) peak, collected with higher statistics, is shown in the Figure 3 inset. From the peak integral breadth, using the Scherrer's equation, it can be estimated that the average size of cobalt crystallites present in the sample was below 5 nm. An accurate determination is hindered by the unfavorable peak-to-background ratio. Since the crystallite size was inferior to the average cluster dimension obtained by AFM, the cobalt clusters had probably a polycrystalline nature. Finally, the film microstructure should consist of a low percentage of nano-sized cobalt clusters embedded into a continuum crystalline thiolate matrix.

Further important structural information about the cobalt-thiolate system can be obtained by differential scanning calorimetry. The DSC-thermograms, recorded on heating the samples, can be interpreted in terms of melting of crystalline regions and thermal decomposition of cobalt-thiolate compounds. When the product was not accurately purified, one additional endothermic peak appeared in the thermograms, due to pure thiol crystals melting. Pure $C_{12}H_{25}SH$ showed a melting temperature of −7 °C, while the Co-$C_{12}H_{25}SH$ product melted in the 33–45 °C temperature range (see Fig. 4a). At low heating rate (1 °C/min), the endothermic peak reveals a double nature: it consists of a large peak with a shoulder at lower temperatures. The two endothermic transitions can be attributed to the melting of crystalline regions produced by the interdigitation of thiol chains (main peak at 33 °C) and to the melting of self-crystallized regions (peak at 45 °C). In a DSC run up to higher temperatures a further endothermic peak appeared at 280 °C. This temperature corresponds to that of the weight loss observed in the TG-thermogram (see Fig. 4b) and, therefore, the endothermic peak can be attributed to the thiol decomposition process. The cooling down of films heated up to 100 °C, showed an exothermic peak produced by the crystallization of thiol-chains. Thus, the crystallization of thiol-chains can occur from both solution and molten phase.

The DSC investigation of Co-$C_{18}H_{37}SH$, showed the presence of a very intense endothermic peak at 62 °C and many peaks at temperature ranging from 100 °C to 160 °C (the pure $C_{18}H_{37}SH$ melting point is 33 °C). These signals can be probably attributed to the melting of crystalline phases trough the interdigitation and self-crystallization of the alkanethiol chains.

The thermal stability of cobalt thiolates at dry state was investigated by Thermogravimetric analysis. When samples of Co-$C_{12}H_{25}SH$ were heated (10 °C/min) under inert atmosphere (fluxing nitrogen), a single weight loss was reproducibly observed in the TG-thermograms at about 260 °C (see Fig. 4b). In particular, the weight of samples started to decrease above 200 °C, with a significant variation in the range 240–280 °C. Such a weight loss was probably produced by the thiolate decomposition and desorption from the cobalt cluster surface. In the case of Co-$C_{18}H_{37}SH$, two weight changes were observed: the first occurred at a temperature of ca. 260 °C and the second at 360 °C. The double weight change was probably caused by the thiol decomposition which occurred according to a dehydrogenation mechanism [1]. When the unpurified product was investigated by TG, a further weight loss was detected in the thermograms due to the evaporation of free thiol molecules present in the samples.

Both Co-$C_{12}H_{25}SH$ and Co-$C_{18}H_{37}SH$ had a hydrophobic nature and consequently they resulted very soluble in aliphatic and aromatic hydrocarbons (*e.g.*, heptane, cyclohexane, benzene), chlorine solvents (*e.g.*, chloroform, carbon-tetrachloride, dichloroethane), and ethers (*e.g.*, diethyl-ether and THF), only moderately soluble in styrene and practically insoluble in esters (*e.g.*, methylmethacrylate), acetone, alcohol, and water. The solubility and dissolution kinetics changed significantly from solvent to solvent and improved with increasing of temperature. The hydrocarbon solutions of Co-$C_{12}H_{25}SH$ presented a characteristic very intense bloody-red color. In order to establish which chemical specie was responsible of such intense coloration, pure cobalt thiolate

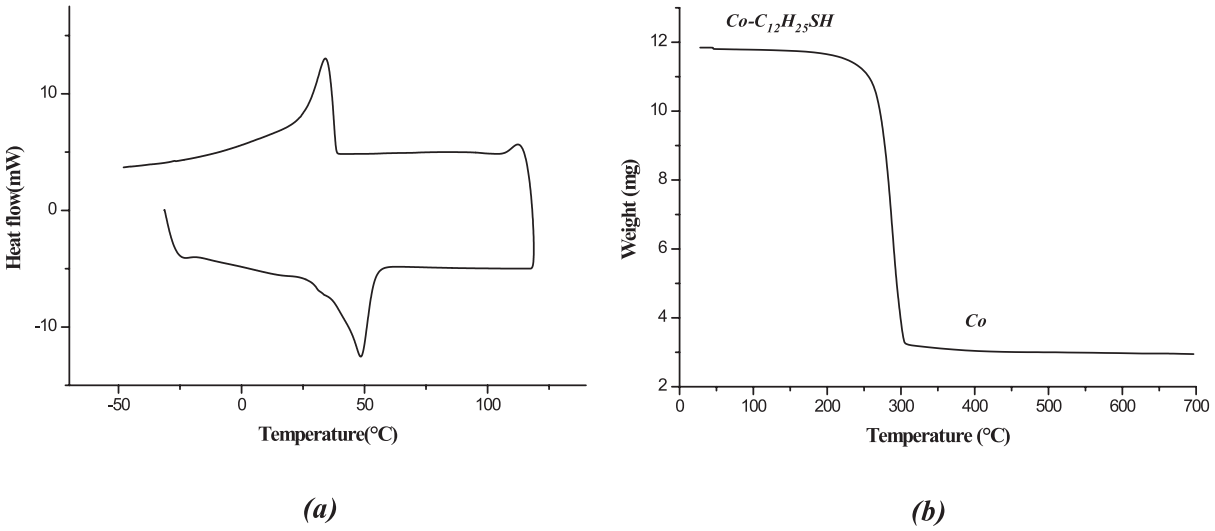

Fig. 4. DSC (a) and TG (b) thermograms of a Co-$C_{12}H_{25}SH$ sample.

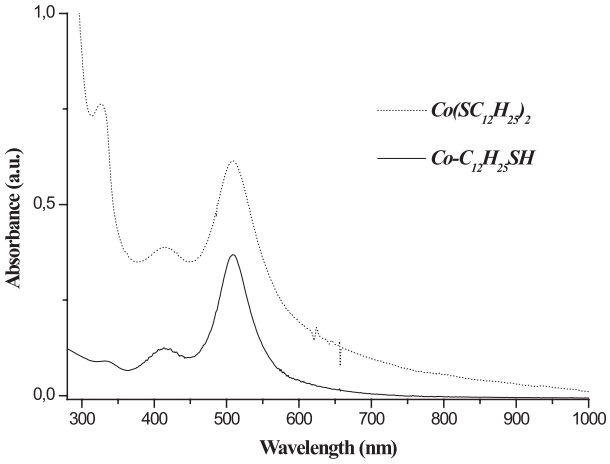

Fig. 5. Comparison between the UV-visible spectra of $Co(SC_{12}H_{25})_2$ and that of an heptane solution of Co-$C_{12}H_{25}SH$.

(*i.e.*, $Co(SC_{12}H_{25})_2$) was produced by an exchange reaction [17]. This is a typically used approach in which $CoCl_2$ is treated with an alkaline alcoholic solution of $C_{12}H_{25}SH$. Slowly the reactive medium appears reddish colored. In Figure 5 the UV-visible spectra of this product is compared with that of an heptane solution of Co-$C_{12}H_{25}SH$. The absorption spectra of the two substances are quite similar pointing to the cobalt-thiolate molecules as the responsible of the intense red color. The UV-visible spectra of Co-$C_{12}H_{25}SH$ solutions were acquired at temperatures ranging from 20 °C to 70 °C and, after cooling down the solution to 20 °C, the UV-visible spectrum perfectly corresponded to the original one, thus indicating a good thermal stability for this product in the explored temperature range. A similar behavior was observed with Co-$C_{18}H_{37}SH$.

In order to investigate the chemical stability of thiolate films to strong acids and alkaline solutions, small pieces of $C_{12}H_{25}SH$ films were dept in absolute sulfuric acid or 1M aqueous NaOH solution. After one month of treatment, the films were recovered, washed in distilled water and dried. In both cases, the films perfectly dissolved in non-polar solvents, producing solutions with the characteristic reddish color. Such result was indicative of a high chemical inertia of these materials.

Standard static NMR experiments in solution have demonstrated a quite large NMR line broadening effect on dodecanethiol-modified Pt nanoclusters [18] and amine- or thiol-capped Au nanoparticles [19,20]. Here, the same trend was found for the Co-$C_{12}H_{25}SH$ system. In fact, as the concentration increased, the static spectra of samples C, B and A became so broad that any useful information was lost. Spectra of diluted samples, performed under the same experimental conditions, showed a certain line width narrowing only at very low concentration (below 1 mg/0.5 ml). The principal cause of such broadening was possibly due to a wide anisotropic distribution of the magnetic susceptibility within the sample. However, this kind of anisotropy can be efficiently averaged out by spinning the sample at the magic angle.

Figure 6 shows ^1H HR-MAS NMR spectra in $CDCl_3$ of three different Co-$C_{12}H_{25}SH$ samples (Figs. 6A, B and C) and of pure $C_{12}H_{25}SH$ (Fig. 6D). A clear broadening of all the signals in the spectra of samples A, B and C with respect to the pure dodecanethiol spectrum of Figure 6D indicated the permanence of some widening mechanisms not suppressed by the magic angle spinning experimental condition. The origin of this residual broadening can lie in discontinuous changes of the magnetic susceptibility at the metal-thiol interface or in some residual dipolar interactions, or in a combination of these effects [21]. Furthermore, we observed that line widths increased as the Co-$C_{12}H_{25}SH$ concentration increased (from Fig. 6C to A). This progressive effect as a function of solute concentration pointed to an increasing interaction (interdigitation) among the thiol chains present in the system.

In Figure 6D the dodecanethiol molecule structure and the corresponding proton resonance assignments are drawn.

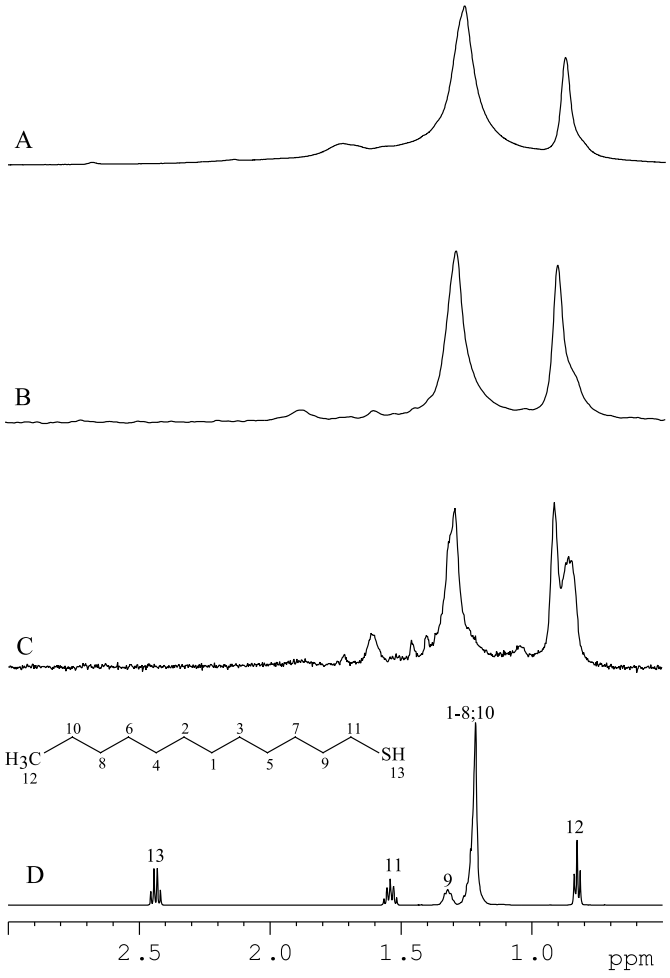

Fig. 6. ^{1}H HR-MAS NMR spectra in $CDCl_3$ of three different Co-$C_{12}H_{25}SH$ samples (A-C) and of pure $C_{12}H_{25}SH$ (D).

The signal of SH groups, which is clearly visible at 2.45 ppm in Figure 6D, practically disappears in the spectra of the Co-$C_{12}H_{25}SH$ system, thus suggesting that almost all the dodecanethiol molecules were bonded to cobalt.

In Figures 6A, B and C the signals in the range 1.2–1.6 ppm arise from the non-equivalent methylene groups of thiol molecules. They appeared to be broader and slightly shifted due to the thiol-cobalt interaction.

The methyl resonance was actually composed of two bands, at 0.84 and 0.89 ppm respectively, whose relative intensities vary with Co-$C_{12}H_{25}SH$ concentration. The line at 0.84 ppm, which had a quite similar chemical shift in the pure dodecanethiol, could be tentatively assigned to the non-interacting thiolate molecules. In fact, the effect of the metal on the chemical shift of the terminal dodecanethiol CH_3 groups bound to cobalt clusters should be relatively small due to their distance [20]. On the other hand, the resonance at 0.89 ppm could be assigned to the interacting chains of both thiolate molecules and passivated cobalt clusters. This is in agreement with the progressive disappearance of the 0.84 ppm signal as the concentration increases and with the diffusion measurements as well.

4 Discussion

Thiols are very good surface modifying agents for metals. The thiol molecules bond the metal surface through a covalent bond (*i.e.*, chemisorption) produced by a red-ox reaction [18]. In addition, long-chain alkane-thiol molecules can self-organize on the metal surface, giving a regular pseudo-solid structure which constitutes an effective diffusion barrier for chemical species. Actually, a number of nucleophylic compounds (*e.g.*, phosphines, ammines) can be adsorbed on metallic surfaces [22], but thiols are the most interesting passivating agent class since of the strong interaction and the large variety of metal substrates that undergo such adsorption. However, depending on the metal nature (*i.e.*, the red-ox potential), the chemical interaction can be limited just to the metal surface, like in the case of Au, Ag, Pd, Pt, etc., or it may consist of an erosive process which gradually dissolves metal thus producing the corresponding thiolate compound (*e.g.*, Hg, Pb, Co, Ni, Cu). Also in the case of very reactive metals, the erosion of the solid surface can be observed only when the reaction product (*i.e.*, the metal thiolate) is soluble in the reactive medium so that it can be progressively removed from the metal surface during the reaction. Since long-chain alkane-thiolate molecules are scarcely soluble in low-molecular weight alcohols (*e.g.*, ethanol) the treatment of metal by alcoholic solutions of thiols usually inhibits their surface erosion. The treatment of reactive metals with absolute thiols or their hydrocarbon solutions, which well dissolve the thiolate layer, is generally cause of a partial metal grain erosion. In the presence of alcoholic solutions of thiols and for reaction performed at room temperature, also reactive metals (*e.g.*, Co, Ni) are not completely converted to cobalt thiolate. Rather, a large amount of metal debris (which surface is saturated by SR-groups), are produced. The size of these metal crystals depends on the erosion extent.

To obtain Co(0) clusters of different sizes, the erosive process should be controlled. This can be performed principally by varying the amount of thiol involved in the chemical treatment. In particular, to avoid the erosive process and obtain just a particle surface coating, a very dilute ethanol solution of thiol (*e.g.*, 2 mmol/cm^3) should be slowly added to the metal suspension (also dilute by ethanol), at room temperature and under moderate stirring to prevent the thiolate layer breaking. An approximate stoichiometric calculation of the thiol quantity required for the saturation of the metal grain surface is possible, because of the high yield of the polyol reduction and the simple geometry characterizing the cobalt grains (*i.e.*, monodisperse spherical particles). Reaction time and temperature are important parameters too. Whereas, the prolonged permanence of cobalt grains in presence of a large excess of thiol can cause quantitative conversion of cobalt particles to cobalt thiolate. Analogously, the heating increases both erosion rate and extent.

The controlled action of dodecanethiol on a micronic cobalt powder results to be of a certain importance since it allows the direct preparation of a new type of nano-structured material. In particular, according to the

microstructure, this material can be classified as a metal-dielectric nanocomposite. In fact, it is made of nanometer-in-size cobalt clusters uniformly dispersed inside a continuum non-metallic matrix. Metal filler size and percentage depend on the erosion extent and, therefore, on the experimental conditions during the metal-thiol reaction. It is well established that, for the ability of RS-groups to bridge-formation, metal thiolates have a polymeric nature. Here, it has been found that long-chain thiolate molecules can produces polymeric structures characterized by a quite good cohesion (*e.g.*, $Co(SC_{12}H_{25})_2$). However, the good cohesion properties which characterize such composite systems are probably related also to the co-crystallization of the alkane-thiol chains bonded to the cluster surface with that of the poly-[$Co(SR)_2$-] form. The Co-$C_{12}H_{25}SH$ system has, for example, a rubbery consistence. Nanocomposites films made by this type of cobalt thiolate are mechanically robust and consequently they can be used for the fabrication of functional devices (*e.g.*, high-density recording media).

Important structural information on the cobalt-based systems are coming also from preliminary diffusion measurements carried out by NMR on Co-$C_{12}H_{25}SH$ samples at different concentrations. In general, a multi-exponential decay of the magnetization as a function of the gradient strength was observed. The average diffusion coefficients of all the lines decreased with the increasing of sample concentration, pointing to a progressive aggregation process. In particular, we found that the band at 0.84 ppm corresponds to one only diffusion coefficient, while the band at 0.89 ppm indicates the presence of two types of diffusing molecules whose diffusion coefficients differs by two orders of magnitude. The fast diffusing molecules associated with the line at 0.89 ppm have diffusion coefficients comparable with those of the molecules associated with the line at 0.84 ppm. Thus, they can be respectively identified as interacting and non-interacting thiolate molecules. On the other hand, the slow diffusing component at 0.89 ppm can be attributed to the nano-sized cobalt clusters.

In agreement with AFM results, the picture emerging from NMR measurements indicate that the film microstructure should consist of nano-sized cobalt clusters and thiolate molecules which produce polymeric structures trough a progressive aggregation process.

5 Conclusions

The thiol-metal reaction is usually limited to a surface chemisorption process. However, because of the high chemical reactivity which characterizes fine solids, micrometric cobalt particles can react with concentrated dodecanethiol and octadecanethiol solutions to produce cobalt thiolate molecules, *i.e.*, $Co(SR)_2$. The reaction is not complete and a large quantity of thiol-derivatized nanocrystalline cobalt clusters (*i.e.*, $Co_n(SR)_m$, with $n \gg m$) result. The nano-sized cobalt clusters have a quasi spherical shape and a broad size distribution. Therefore, the final product is a nano-composite material made of cobalt nano-crystals embedded into a continuum cobalt thiolate matrix. For the ability of RS-group to bridge-formation, cobalt thiolate have a polymeric nature and, depending on the type of thiol used, the resulting nanocomposite materials can be characterized by a waxy (octadecanethiol) or a rubbery (dodecanethiol) consistency. In addition, these materials have a high hydrophobic nature, are stable to strong acid and alkaline solutions and are very intensely red colored due to the cobalt thiolate presence. The investigated cobalt-based systems (*i.e.*, Co-$C_{12}H_{25}SH$ and Co-$C_{18}H_{37}SH$) are crystalline, quite thermally stable (decomposition temperature of about 300 °C), and able to produce extended polymeric structures when dissolved into non-polar organic solvents.

References

1. C.M. Friend, D.A. Chen, Polyhedron **16**, 3165 (1997)
2. Z.L. Wang, Mater. Charact. **42**, 101 (1999)
3. *Physics and Chemistry of Metal Cluster Compounds*, edited by L.J. de Jongh (Kluwer Academic Publishers, Dordrecht Hardbound, 1994)
4. K. Puech, W.J. Blau, J. Nanopart. Res. **3**, 13 (2001)
5. N.A.F. Al-Rawashdeh, M.L. Sanfrock, C.J. Seugling, C.A. Foss, J. Phys. Chem. **102**, 361 (1998)
6. J.C. Wittmann, P. Smith, Nature **352**, 414 (1991)
7. A.H. Lu, G.H. Lu, A.M. Kessinger, C.A. Foss, J. Phys. Chem. B **101** (45), 9139 (1997)
8. L. Zimmerman, M. Weibel, W. Caseri, U.W. Suter, J. Mater. Res. **8**, 1742 (1993)
9. M. Weibel, W. Caseri, U.W. Suter, H. Kiess, E. Wehrli, Polym. Adv. Tech. **2**, 75 (1991)
10. L. Zimmerman, M. Weibel, W. Caseri, U.W. Suter, P. Walther, Polym. Adv. Tech. **4**, 1 (1992)
11. A.H. Lu, G.H. Lu, A.M. Kessinger, C.A. Foss, J. Phys. Chem. B **101**, 9139 (1997)
12. K. Baba, F. Takase, M. Miyagi, Optics Comm. **139**, 35 (1997)
13. *Fine Particles Synthesis, characterization, and mechanism of growth*, edited by T. Sugimoto (Marcel Dekker, Inc., New York, 2000), pp. 460–496
14. S.J. Gibbs, C.S. Jr. Johnson, J. Magn. Reson. **93**, 395 (1991)
15. C.S. Jr. Johnson, Progr. NMR Spectr. **34**, 203 (1999)
16. R. Mills, J. Phys. Chem. **77**, 685 (1973)
17. United States Patent N° 4,148,813 (1979); United States Patent N° 4,148,815 (1979); United States Patent N° 4,148,816 (1979)
18. X. Fu, Y. Wang, N. Wu, L. Gui, Y. Tang, J. Colloid Interface Sci. **243**, 326 (2001)
19. D.V. Leff, L. Brandt, J.R. Heath, Langmuir **12**, 4723 (1996)
20. M.J. Hostetler, J.E. Wingate, C.-J. Zhong, J.E. Harris, R.W. Vachet, M.R Clark, J.D. Londono, J.S. Green, J.J. Stokes, G.D. Wignall, G.L. Glish, M.D. Porter, N.D. Evans, R.W. Murray, Langmuir **14**, 17 (1998)
21. R.H. Terril, T.A. Postlethwaite, C.-H. Chen, C.-D. Poon, A. Terzis, A. Chen, J.E. Hutchinson, M.R. Clark, G. Wignall, J.D. Londono, R. Superfine, M. Falvo, C.S. Jr. Johnson, E.T. Samulski, R.W. Murray, J. Am. Chem. Soc. **117**, 12537 (1995)
22. J.L. Whitten, H. Yang, Surf. Sci. Rep. **24**, 55 (1996)